Volumetric Curvature-Attribute Applications for Detection of Fracture Lineaments and their Calibration

By Satinder Chopra, Kurt J. Marfurt
Arcis Corporation, Calgary; University of Houston, Houston

Introduction

Computation of volumetric curvature is a significant advancement in the field of attributes. Until recently, curvature attribute applications were limited to interpreted horizons. Horizon-based curvature has been successfully used in the prediction of fault and fractures, and has been shown to be correlated with open fractures measured on outcrops (Lisle, 1994) or measured by production tests (Hart et al., 2002). Horizon-based curvature is limited not only by the interpreter's ability to pick, but also the existence of horizons of interest at the appropriate level in 3D seismic data volumes. Horizon picking can be a challenging task in datasets contaminated with noise and where rock interfaces do not exhibit a consistent impedance contrast amenable to human interpretation. Very recently, volumetric computation of curvature has been introduced, which dispels the need for consistent horizons in the zone of interest (Al-Dossary and Marfurt, 2006). By first estimating the volumetric reflector dip and azimuth that represents the best single dip for each sample in the volume, followed by computation of curvature from adjacent measures of dip and azimuth, a full 3D volume of curvature values is produced. There are many curvature measures that can be computed, but the most-positive and most-negative curvature measures are the most useful in that they tend to be most easily related to geologic structures. Volumetric curvature attributes are valuable in mapping subtle flexures and folds associated with fractures in deformed strata. In addition to faults and fractures, stratigraphic features such as levees and bars and diagenetic features such as karst collapse and hydrothermally altered dolomites also appear to be well-defined on curvature displays. Channels appear when differential compaction has taken place.

An interesting feature of their approach is the multi-spectral curvature computation that can yield both long wavelength and short wavelength curvature estimates, which enhance geologic features having different scales. Curvature images having different wavelengths provide different perspectives of the same geology (Bergbauer et al., 2003). Tight (short-wavelength) curvature often delineates details within intense, highly localized fracture systems. Broad (long wavelength) curvature often enhances subtle flexures on the scale of 100-200 traces that are difficult to see in conventional seismic, but are often correlated to fracture zones that are below seismic resolution, as well as to collapse features and diagenetic alterations that result in broader bowls. Al-Dossary and Marfurt (2006) compute multispectral estimates of volumetric curvature using a 'fractional derivative' approach. They define the fractional derivative as

$$\frac{\partial^\alpha u}{\partial x^\alpha} = F^{-1}\left[-i(k_x)^\alpha F(u) \right] \qquad \text{eq. 1}$$

where the operators F and F^{-1} denote the forward and inverse Fourier transform, where u is an inline or crossline component of reflector dip, and where α is a fractional real number that typically ranges between 1 (giving the first derivative) and 0 (giving the Hilbert transform) of the dip. The nomenclature 'fractional derivative' was borrowed from Cooper and Cowans (2003); however, an astute mathematician will note that the i is not in the parentheses. In this manner we can interpret equation 1 as simply a low pass filter of the form $k_x^{(\alpha-1)}$ applied to a conventional first derivative.

The space domain operators corresponding to different values of α mentioned above are convolved with the previously computed dip components estimated at every sample and trace within the seismic volume. In addition, the directional derivative is applied to a circular rather than linear window of traces, thereby avoiding a computational bias associated with the acquisition axes. Lower values of α decrease the contribution of the high wavenumbers, thereby shifting the bandwidth towards longer wavelength. Thus full 3D curvature attribute volumes are available for analysis at different scales, which helps extract meaningful and subtle information from seismic data.

Examples

In Figure 1a we show a segment of a seismic section from a 3D volume from south-central Alberta, Canada, with a horizon tracked over it. Some seismic signatures

continued on page 24

Volumetric Curvature-Attribute Applications for Detection of Fracture Lineaments and their Calibration - *continued*

continued from page 23

of faults are seen along this horizon. In Figure 1b and d, we show the most-positive and most-negative curvature attributes computed directly from these horizon picks. Notice that while the NW-SE fault patterns are seen on these displays, we also see an imprint of the acquisition footprint (indicated in the blue and green ellipses), which are artifacts of such a computation. In Figures 1c and 1e, we show the most-positive and most-negative curvature attributes extracted along the horizon in question from the most-positive and most-negative curvature volumes. Notice that the fault lineaments are better focused and well defined while the artifacts seen in Figures 1b and d are suppressed. Volumetric estimates of dip and azimuth are performed using overlapping analysis windows (+/- 10 ms and 9 traces for this example) which are less sensitive to backscattered ground roll than calculating the dip and azimuth from the picking of peaks and troughs. Volumetric measures of seismic coherence or trace similarity is a well-established means of mapping lateral discontinuities in seismic waveforms. In Figure 2a we show a coherence strat cube shown intersected with a seismic random line AA' indicated in Figures 1b to e. A strat-cube is a sub-volume of seismic data or its attributes, bounded by two horizons which may not necessarily be parallel or covering seismic data above and/or below a given horizon. Since the top face of the coherence strat-cube corresponds to the blue

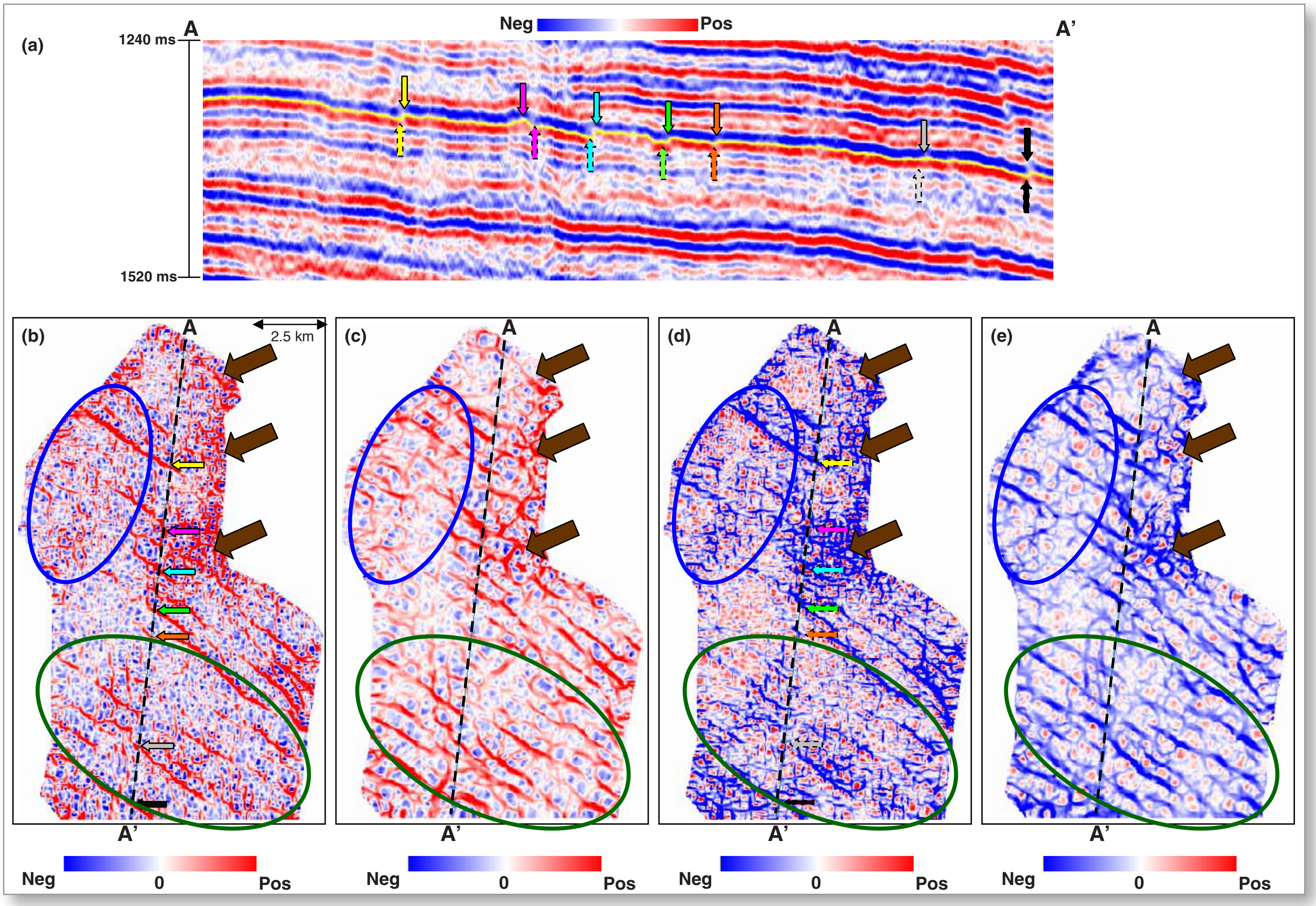

Figure 1. (a) An arbitary dip line AA' (shown dotted in Figure 1b) showing a picked horizon (in yellow). Most-positive curvature (b) computed directly from the horizon picks and (c) extracted along the horizon from the most-positive curvature attribute volume. Most-negative curvature (d) computed directly from the horizon picks, and (e) extracted along the horizon from the most-negative curvature attribute volume. Notice the inline and crossline artifacts seen on the curvature images computed directly from the horizon picks which are not seen on the attributes extracted along the horizon from the curvature attribute volumes.

continued on page 25

Volumetric Curvature-Attribute Applications for Detection of Fracture Lineaments and their Calibration - *continued*

continued from page 24

high amplitude picked horizon troughs, it appears as high coherence (white), except for the prominent faults (black). Minor faults which result in offsets significantly less than a seismic wavelet, or that are otherwise poorly resolved or even smeared by seismic imaging appear to be continuous and are not seen in this coherence volume. In contrast, curvature volumes measure a different property of the seismic data – that of structural deformation. The reason that we see small 'faults' on curvature volumes can be due to geology (the discontinuous 'fault' is actually a continuous flexure), seismic resolution (the fault displacement is considerably less than a seismic wavelet), or data quality (inaccurate seismic imaging). Figures 2b and c show the most-positive curvature (long-wavelength) and most-positive curvature (short-wavelength) strat-cubes intersected by an arbitrary dip line AA'. Notice, while the long-wavelength display provides the broad definition of such features, the short-wavelength version provides the finer definition of the individual lineaments. Both the prominent as well as the weaker looking red lineaments correlate nicely with the localized highs seen on the trough of the picked horizon. Similarly, Figures 2d and

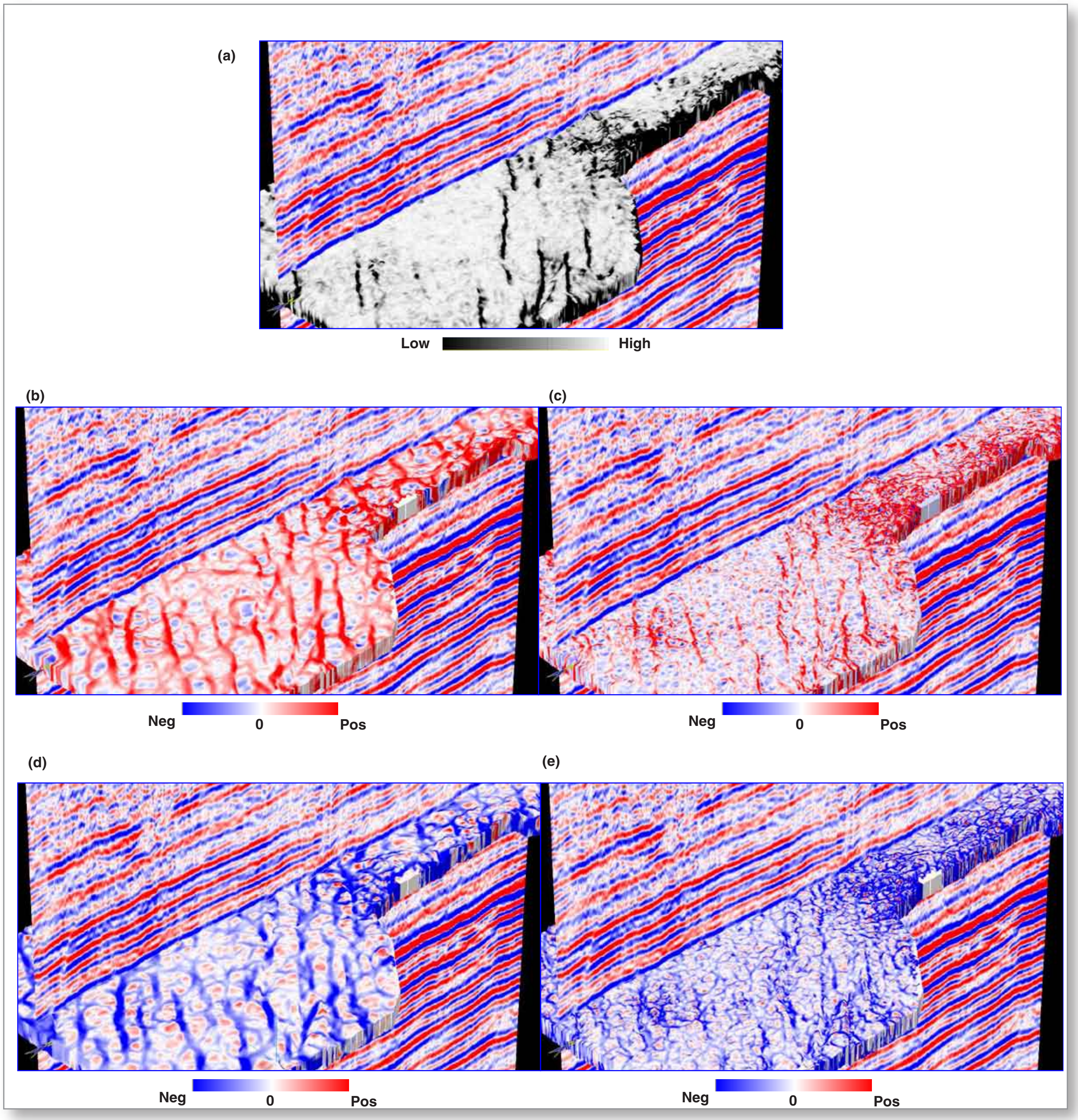

Figure 2. Zoom of chair-displays where the vertical display is a portion of the dip line AA' shown in Figure 1 through the original 3D seismic amplitude volume while the horizontal displays are strat slices through (a) coherence (b) most-positive (long-wavelength) (c) most-negative (long-wavelength) (d) most-positive (short-wavelength) attribute volumes. The fault lineaments correlate with the upthrown and downthrown signatures on the seismic.

continued on page 26

Volumetric Curvature-Attribute Applications for Detection of Fracture Lineaments and their Calibration - *continued*

continued from page 25

e show the most-negative curvature (long-wavelength) and most-negative curvature (short-wavelength) strat-cubes being intersected by line AA'. Both the prominent as well as the weaker looking blue lineaments correlate nicely with the localized lows seen on the horizon reflection, as is expected.

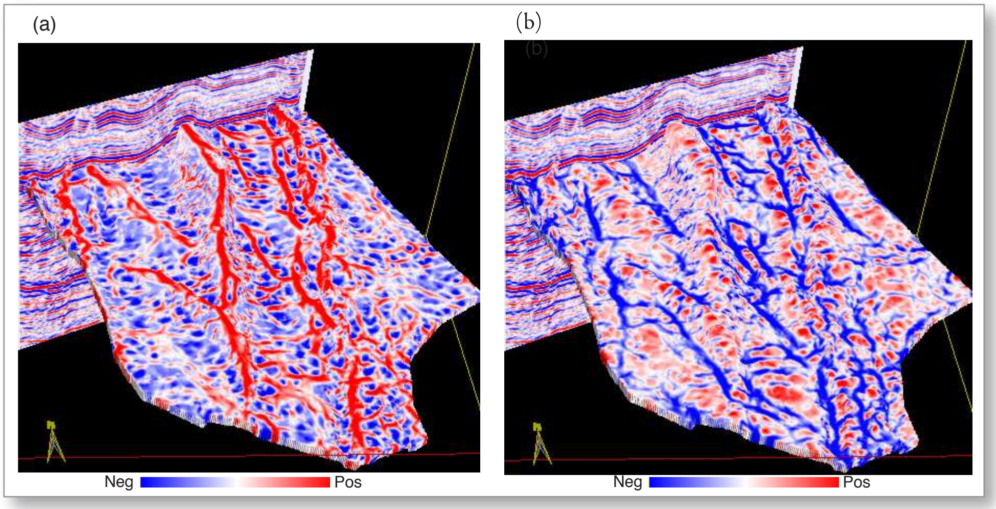

Figure 3. (a) Most-positive curvature and (b) most-negative curvature strat-slices 30 ms below a tracked horizon surface extracted from corresponding curvature volumes. The size of the survey displayed is 100 sq. km. (Data courtesy: Arcis Corporation, Calgary)

In Figure 3a we show a strat-slice display of the most-positive curvature volume from north-east British Columbia, 30 ms below a prominent trackable horizon. The surface displayed is close to 1200 ms. The horizon at this level is not easy to track and so the attribute volume helps in studying the fault patterns at this level. Similarly, the equivalent strat-slice extracted from the most-negative curvature volume is shown in Figure 3b. Notice the fault patterns can be clearly seen at this level though the horizon is not easy to pick. In Figure 4 we show a zoomed image of strat-cube displays of

continued on page 27

Volumetric Curvature-Attribute Applications for Detection of Fracture Lineaments and their Calibration - *continued*

continued from page 26

(a) long-wavelength and (b) short-wavelength versions of a fault/fracture system from British Columbia, intersecting a seismic inline. The surface displayed is close to 1600 ms. Notice that the red peaks (Figures 4a and b) on the fault lineaments (running almost north-south) correlate with the upthrown signature on seismic.

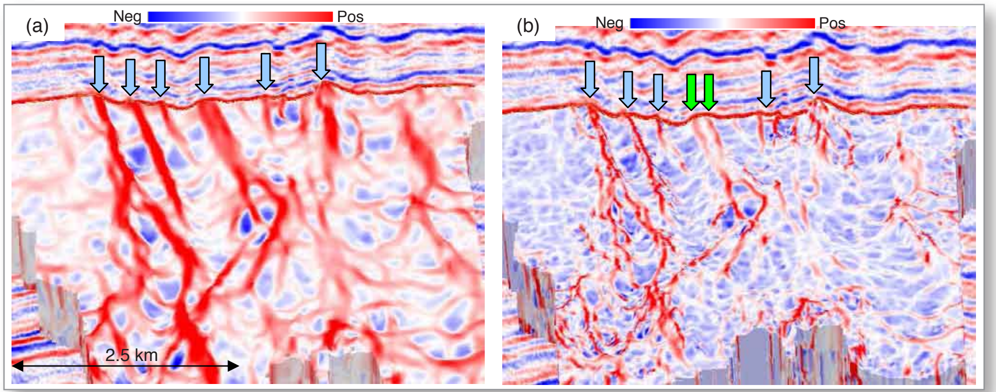

Figure 4. (a) Most-positive curvature (long wavelength) and (b) most-positive curvature (short wavelength), strat-slices one sample below the tracked horizon surface extracted from corresponding curvature volumes. Notice the higher resolution and the crisp display of the different faults seen on the strat-slice. (Data courtesy: Arcis Corporation, Calgary).

While a direct prediction of open fractures using curvature attributes requires a significant amount of calibration through the use of production, tracer, image log or microseismic measurements, volumetric curvature attribute analysis serves as a powerful aid to such structural interpretation. Such fault/fracture interpretation has been ably supplemented with a calibration procedure with well log data, in that the orientations of the fault/fracture lineaments interpreted on curvature displays can be combined in the form of rose diagrams, which in turn can be compared with similar diagrams obtained from FMI (Formation Micro-Imager) wells logs to gain confidence in calibration. Figure 5a shows a time surface from a 3D seismic volume from northern Alberta, Canada. A great number of faults can be seen trending N-S, while a fewer number faults trend NE-SW and E-W. In Figure 5b we show the individual fault/fracture lineaments tracked in yellow color. The orientations of these lineaments have been combined in the form of a rose diagram shown in Figure 5c, retaining the color of the lineaments. As stated above these rose diagrams can be compared with similar rose diagrams that are generated from image logs.

Conclusions

Volumetric curvature attributes are valuable for prediction of fracture lineaments in deformed strata. Besides faults and fractures, stratigraphic features also appear to be well-defined on curvature displays.

Multispectral volumetric curvature attributes are valuable for prediction of fracture lineaments in deformed strata. Several applications of volume curvature have been

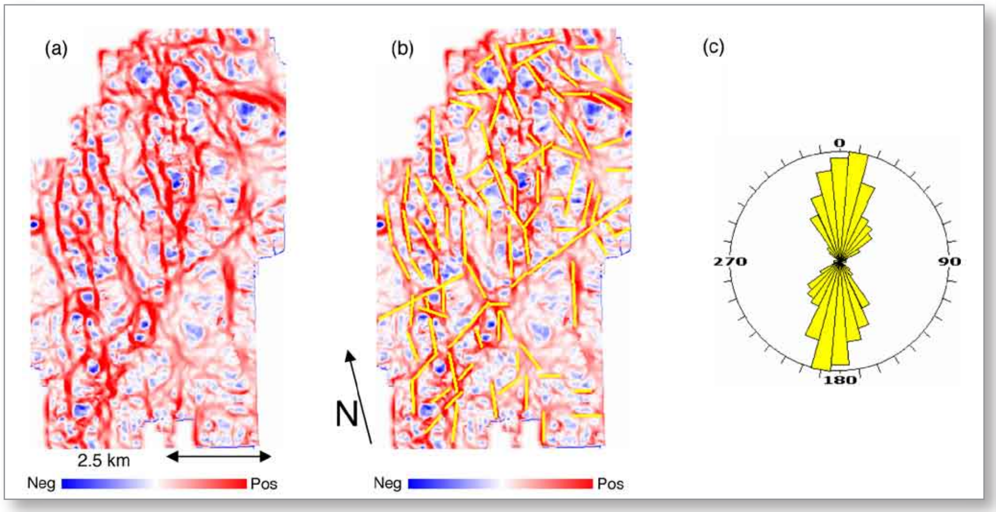

Figure 5. (a) A strat-slice through the most-positive curvature (long wavelength) volume and (b) the interpretation of lineaments corresponding to subtle faults carried out on the slice in (a). Rose diagram prepared for the set of lineaments shown in (b) is shown in (c), and can be compared with similar rose diagrams available from image logs. (Data courtesy: Arcis Corporation, Calgary)

continued on page 28

Volumetric Curvature-Attribute Applications for Detection of Fracture Lineaments and their Calibration - *continued*

continued from page 27

completed in different geological settings, which are found to be useful in imaging different stratigraphic features, ranging from channel boundaries, through broad flexures, to small scale faults and highly fractured zones.

Acknowledgements

We wish to thank Arcis Corporation for permission to publish and present this work.

References

Al-Dossary, S., and K. J. Marfurt, 2006, Multispectral estimates of reflector curvature and rotation: Geophysics, 71, P41-P51.

Bergbauer, S., T. Mukerji, and P. Hennings, 2003, Improving curvature analyses of deformed horizons using scale-dependent filtering techniques: AAPG Bulletin, 87, 1255-1272.

Chopra, S. and Marfurt, K. J., 2007, Multispectral volumetric curvature adding value to 3D seismic data interpretation, CSPG/CSEG Convention, Calgary.

Cooper, G. R. J., and D. R. Cowans, 2003, Sunshading geophysical data using fractional order horizontal gradients, The Leading Edge, 22, 204-205.

Hart, B.S., R. Pearson, and G. C. Rawling, 2002, 3-D seismic horizon-based approaches to fracture-swarm sweet spot definition in tight-gas reservoirs: The Leading Edge, 21, 28-35.

Lisle, R. J., 1994, Detection of zones of abnormal strains in structures using Gaussian curvature analysis: AAPG Bulletin, 78, 1811-1819.

Marfurt, K. J., 2006: Robust estimates of reflector dip and azimuth: Geophysics, 71, P29-P40.